Phosphoregulation of sorting signal–VHS domain interactions by a direct electrostatic mechanism

Yukio Kato[1,2], Saurav Misra[2,3], Rosa Puertollano[1], James H. Hurley[3] and Juan S. Bonifacino[1]

[1]*Cell Biology and Metabolism Branch, National Institute of Child Health and Human Development, National Institutes of Health, Bethesda, Maryland 20892, USA.* [2]*These authors contributed equally to this work.* [3]*Laboratory of Molecular Biology, National Institute of Diabetes and Digestive and Kidney Diseases, National Institutes of Health, Bethesda, Maryland 20892, USA.*

Published online: 28 May 2002, doi:10.1038/nsb807

Phosphorylation of the cytosolic tails of transmembrane receptors can regulate their intracellular trafficking. The structural basis for such regulation, however, has not been explained in most cases. The cytosolic tail of the cation-independent mannose 6-phosphate receptor contains a serine residue within an acidic-cluster dileucine signal that is important for the function of the receptor in the biosynthetic sorting of lysosomal hydrolases. We show here that phosphorylation of this Ser enhances interactions of the signal with its recognition module, the VHS domain of the GGA proteins. Crystallographic analyses demonstrate that the phosphoserine residue interacts electrostatically with two basic residues on the VHS domain of GGA3, thus providing an additional point of attachment of the acidic-cluster dileucine signal to its recognition module.

The biosynthetic sorting of soluble hydrolases to lysosomes is carried out by two transmembrane receptors: the cation-independent mannose 6-phosphate receptor (CI-MPR) and the cation-dependent mannose 6-phosphate receptor (CD-MPR)[1]. The hydrolases bind *via* mannose 6-phosphate groups to the luminal domains of both mannose 6-phosphate receptors (MPRs) in the *trans*-Golgi network (TGN). The cytosolic tails of both MPRs contain acidic-cluster dileucine signals[2–6] (Fig. 1*a*) that interact with the VHS (Vsp27p/Hrs/STAM) domains of the GGA (Golgi-localized, γ-ear-containing, ADP-ribosylation-factor-binding) adaptor proteins GGA1, GGA2 and GGA3 (refs 7–9). These interactions mediate incorporation of the MPRs into clathrin-coated vesicles budding from the TGN[7,10]. The vesicles deliver the receptors and their cargo to endosomes, where the acidic luminal pH induces dissociation of the hydrolases from the MPRs. The enzymes then proceed to lysosomes with the fluid phase, while the receptors return to the TGN for further rounds of sorting[1].

Several lines of evidence suggest that phosphorylation of a Ser residue contained within the acidic-cluster dileucine signal of the CI-MPR (DDS**D**EDLLHI; residues are numbered relative to Asp 0, indicated in bold) could regulate recognition of the signal at the TGN. This Ser residue, referred to as Ser (-1), is in a sequence context that fits the (Ser/Thr)XX(Asp/Glu) consensus motif for phosphorylation by casein kinase II (CKII), in which the X residues are most often acidic[11]. Ser (-1) can be phosphorylated *in vitro* by purified CKII[12] or a CKII-like enzyme associated with clathrin-coated vesicles[13], as well as *in vivo*[12–14]. Systematic mutational analyses of the CI-MPR signal have demonstrated that replacement of Ser (-1) with an Ala residue impairs sorting of lysosomal hydrolases[6]. These observations are consistent with a possible role for Ser (-1) phosphorylation in the regulation of CI-MPR sorting.

The crystal structures of the VHS domain of GGA3 in complex with unphosphorylated CI- and CD-MPR signal peptides[15] and of the VHS domain of GGA1 with the unphosphorylated CI-MPR signal[16] revealed the key determinants for the binding of the core acidic-cluster dileucine motif to be Asp 0, Leu 3 and Leu 4. The acidic cluster is present in all of the receptor tail sequences known to bind GGA VHS domains[7–9,17] (Fig. 1*a*), yet only one of the acidic residues (Asp 0) forms a strong structural interaction with the VHS domain[15,16]. In the CI-MPR signal in complex with the GGA1 and GGA3 VHS domains, the acidic residues Asp (-3) and Asp (-2) are disordered, and the side

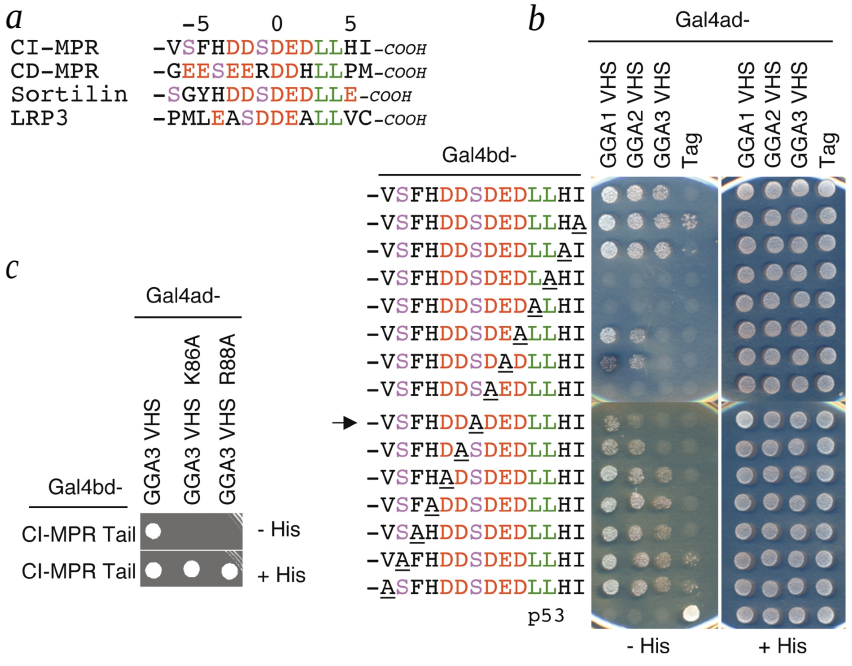

Fig. 1 Yeast two-hybrid analyses reveal a role for a Ser residue of the CI-MPR tail in interactions with GGA VHS domains. ***a***, C-terminal sequences of the CI-MPR, CD-MPR, sortilin and LDL receptor related protein 3 (LRP3) tails containing acidic-cluster dileucine signals. Acidic residues, the critical dileucine pair and serine residues are highlighted in red, green and magenta, respectively. Residues are numbered relative to Asp 0. ***b***, Yeast cells were co-transformed with plasmids encoding: (i) Gal4bd fused to CI-MPR tail constructs having the C-terminal sequences indicated on the left or p53 (in pGBT9) and (ii) GAL4ad fused to the VHS domains of GGA1, GGA2 or GGA3, or the T antigen (Tag) (in pGAD424). Ala substitutions are underlined. ***c***, Yeast cells were co-transformed with: (i) plasmids encoding Gal4bd fused to the normal CI-MPR tail (in pGBT9) and (ii) GAL4ad fused to the GGA3 VHS domain or the K86A or R88A mutants of this domain (in pGAD424). Co-transformed cells were spotted onto plates lacking leucine and tryptophan, with or without histidine (+His and –His, respectively), and incubated at 30 °C. Growth on –His plates is indicative of interaction. In (*b*), notice the decreased interaction with the three VHS domains of the S(-1)A mutant (arrow).

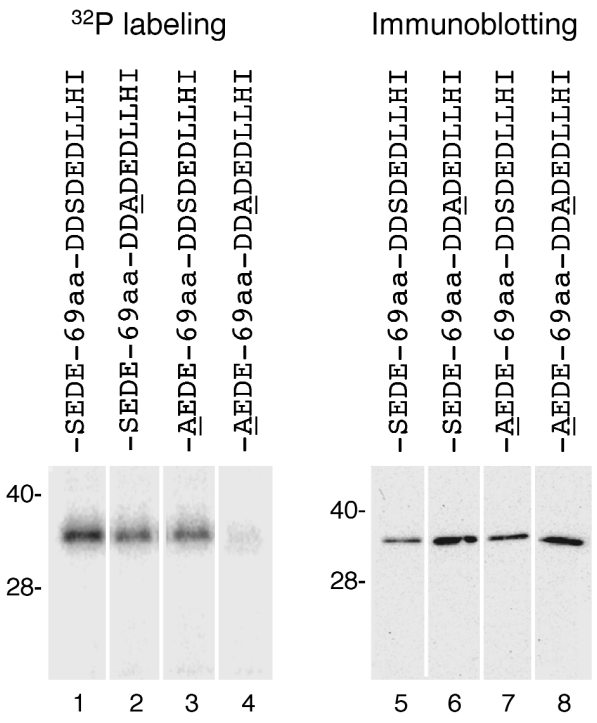

Fig. 2 Phosphorylation of the CI-MPR tail in yeast. Yeast cells expressing the Gal4bd–HA–CI-MPR constructs indicated in the figure were metabolically labeled for 3 h with [32P]orthophosphate. After dilution of cell extracts with 50 mM Tris-HCl, pH 7.5, 150 mM NaCl, 0.1 mM EDTA and 0.5% (v/v) Tween 20, proteins were isolated by immunoprecipitation with an antibody to the HA-tag (Covance). Immunoprecipitates were analyzed by SDS-PAGE and autoradiography. 32P-labeled proteins were detected by autoradiography (lanes 1–4) and protein expression was revealed by immunoblotting with an antibody to the HA epitope (lanes 5–8). The positions of molecular mass markers (in kDa) are indicated on the left.

chains of Glu 1 and Asp 2 point away from the VHS domain[15,16]. The structures do not reveal the presence of well-defined pockets on the VHS surface that could be occupied by the additional acidic residues. The inference can be drawn from the structure that the acidic cluster may be conserved partly to provide a CKII recognition site, as opposed to interacting with basic regions on the GGA VHS domain. We, therefore, set out to examine the possibility that CKII phosphorylation regulates the association of the CI-MPR and GGA proteins.

Phosphorylation enhances binding

We began by performing a systematic alanine scanning mutagenesis and yeast two-hybrid analysis of the acidic-cluster dileucine signal of CI-MPR to determine the requirement of specific residues for interactions with GGA VHS domains. As predicted from previous structural data[15,16], substitution of Asp 0, Leu 3 or Leu 4 residues completely abrogated interactions of the CI-MPR signal with the VHS domains of the three GGAs (Fig. 1*b*). Interestingly, replacement of Ser (-1) decreased interactions with the three GGA VHS domains (Fig. 1*b*) despite the very limited interactions observed with this residue in the crystal structure. We inferred that this requirement for Ser (-1) is likely due to its phosphorylation by yeast CKII, which has substrate specificity similar to mammalian CKII[18]. Metabolic labeling with [32P]orthophosphate and immunoprecipitation of yeast cells expressing the Gal4-binding domain (Gal4bd) appended with the CI-MPR-tail demonstrated that this fusion protein is indeed phosphorylated *in vivo* (Fig. 2, lane 1). Mutation of S(-1)A partially decreased phosphorylation (Fig. 2, lane 2). Another Ser residue located 76 residues N-terminal to Asp 0 is also known to be phosphorylated by CKII both *in vitro* and *in vivo* in mammalian cells[13,14]; however, mutation of this Ser does not affect sorting[6] or interactions with the GGA VHS domains (data not shown). Mutation of Ser (-76) also caused a partial decrease of phosphorylation in the yeast cells (Fig. 2, lane 3). Finally, mutation of both Ser (-1) and Ser (-76) completely abolished phosphorylation of the fusion protein (Fig. 2, lane 4), thus demonstrating that these two Ser residues in the CI-MPR tail are the only phosphorylation sites on the fusion protein. Phosphorylation of Ser (-1) could, therefore, explain the requirement of this residue for optimal interactions with the GGA VHS domains in the yeast two-hybrid assays.

To assess more directly the effect of CKII-mediated phosphorylation of the signal on its interactions with GGA VHS domains, we performed GST pull-down assays (Fig. 3*a*). Recombinant GGA3 VHS bound to a GST–CI-MPR-tail construct (Fig. 3*a*, lane 1) but not to a construct of the lysosomal membrane protein, GST–Limp-II-tail, used as a negative control (Fig. 3*a*, lane 7). Pretreatment with purified human CKII increased binding by approximately four-fold (Fig. 3*a*, lane 2). This increase was abolished by addition of heparin, a competitive inhibitor of CKII (Fig. 3*a*, lane 3), or by the S(-1)A mutation (Fig. 3*a*, lane 5). The effect of Ser (-1) phosphorylation on interactions was further characterized by isothermal titration calorimetry. Phosphorylated (pCI-MPR; FHDDpSDEDLLHI) and unphosphorylated peptides (CI-MPR; FHDDSDEDLLHI) were tested for binding to purified recombinant VHS domains from GGA1 and GGA3. The phosphorylated peptide bound more strongly to both GGA1 VHS and GGA3 VHS domains than the unphosphorylated peptide (Fig. 3*b*). Phosphorylation of the peptide caused the equilibrium dissociation constant, K_d, to decrease from 7.9 μM to 2.3 μM for the GGA1 VHS domain and from 10.9 μM to 3.5 μM for the GGA3 VHS domain (Fig. 3*c*). Thus, the results of various interaction analyses demonstrate that phosphorylation of Ser (-1) increases the affinity of the CI-MPR signal for GGA VHS domains.

Structural basis for phosphoregulation

To determine the structural basis for the increase in affinity, the GGA3 VHS domain was co-crystallized with the pCI-MPR signal peptide. The crystals grew in space group $C222_1$. The structure was solved by Fourier difference analysis with respect to the GGA3–CD-MPR complex[15] and refined to R_{free} = 0.255 and R_{work} = 0.211 at 2.3 Å resolution.

The pCI-MPR peptide binds between helices 6 and 8 in the same overall conformation as the CI-MPR peptide (Fig. 4*a–d*). The well-ordered central parts of the peptides superimpose with an r.m.s. deviation of 0.53 Å with CD-MPR in the same space group and 0.48 Å with the unphosphorylated CI-MPR in space group $P2_12_12$ (Cα positions Asp 0–Ile 6). The VHS domain is virtually unchanged, with an r.m.s. deviation of 0.27 Å with the unphosphorylated CD-MPR complex in the same space group and 0.64 Å with the CI-MPR determined in $P2_12_12$.

The presence of the pSer phosphate in the crystallized peptide was unambiguous as the highest peak in a difference map that was phased with an atomic model built before the inclusion of the phosphate. The position of the main chain of the peptide at pSer (-1) is virtually unchanged (Fig. 4*d*). The pSer phosphate

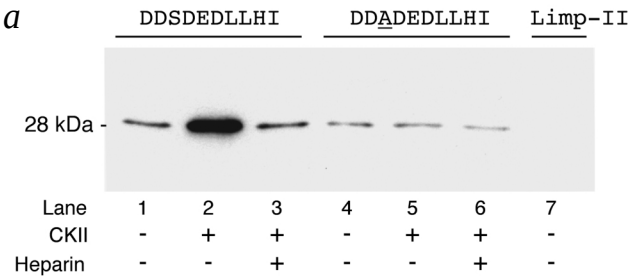

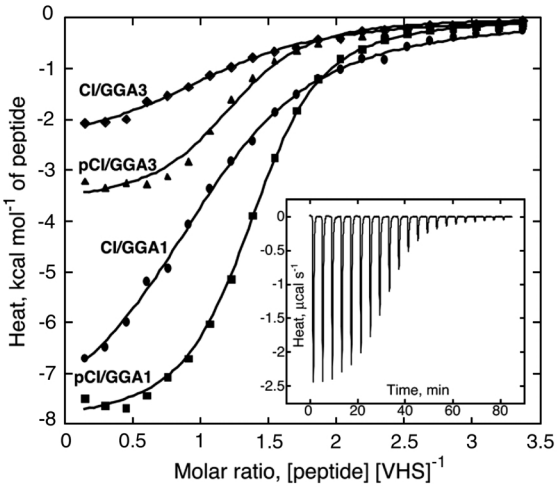

Fig. 3 Phosphorylation enhances binding of the CI-MPR tail to the GGA3 VHS domain *in vitro*. ***a***, Recombinant His_6–GGA3-VHS was tested for interactions with GST fusion proteins bearing the cytosolic tail sequences indicated on top. Some of the GST fusion protein samples were subjected to phosphorylation by recombinant CKII in the absence or presence of heparin, as indicated in the figure. The GST fusion proteins were collected by incubation with glutathione–Sepharose, and the bound His_6–GGA3-VHS was resolved by SDS-PAGE and detected by immunoblotting with anti-His_6. Notice the increased binding of His_6–GGA3-VHS to the GST–CI-MPR tail construct upon treatment with CKII (lane 2). ***b***, Isothermal titration calorimetry measuring the affinities of unphosphorylated CI-MPR (CI) and phosphorylated CI-MPR (pCI) peptides for GGA1-VHS and GGA3-VHS domains. Inset: Differential heat released when 1 mM pCI-MPR peptide is injected into 50 μM GGA1-VHS. The trace is shown after subtraction of data from injection of pCI-MPR into a buffer blank. ***c***, K_d and n (stoichiometry) for the different peptide–VHS domain interactions expressed as the mean ± s.d.

c

Peptide	VHS	K_d (μM)	n
pCI-MPR	GGA1	2.3 ± 0.4	1.3 ± 0.1
CI-MPR	GGA1	7.9 ± 1.0	1.1 ± 0.1
pCI-MPR	GGA3	3.5 ± 0.8	0.9 ± 0.1
CI-MPR	GGA3	10.9 ± 1.1	1.1 ± 0.1

interacts electrostatically with Lys 86 and Arg 88 (Fig. 4*c*), which are conserved in all the GGAs. The interaction with Arg 88 uses both the Nη nitrogens of the guanidino group but only one of the three phosphate oxygens. The two basic residues do not undergo large conformational changes on phosphate binding (Fig. 4*d*). The Lys 86 Nζ moves 0.5 Å, and the Arg 88 Cζ moves 1.0 Å compared to the CD-MPR complex. The shifts are larger relative to the unphosphorylated CI-MPR complex (1.5 and 1.2 Å, respectively), but part of the difference is accounted for by the difference in crystal packing. Thus, receptor phosphorylation does not seem to induce substantial conformational changes in either the signal peptide or the VHS domain. The main consequence of phosphorylation is the introduction of electrostatic interactions with two basic residues that are not present in the unphosphorylated state of the receptor tail.

The importance of Lys 86 and Arg 88 in the GGA3 VHS domain for interactions with the CI-MPR signal was corroborated experimentally using the yeast two-hybrid system. We observed that mutation of either basic residue to Ala abrogated interaction with the CI-MPR signal (Fig. 1*c*), similar to the effect of the S(-1)A mutation in the signal (Fig. 1*b*).

VHS as a phosphoserine-binding module?

The finding that phosphoregulation enhances the binding of the CI-MPR to GGA VHS domains places the VHS domain within a larger class of phosphoserine/phosphothreonine-binding modules, which includes the 14-3-3, WW and FHA (Forkhead-associated) domains[19,20]. The structure of the group IV WW domain from Pin1 bound to a pSer-containing peptide[21] showed that the pSer residue is a central anchor point and the pSer phosphate makes contact with the WW domain through all three nonbridging oxygens. Unphosphorylated peptides have negligible binding to the Pin1 WW domain, consistent with the core role for pSer/pThr. The FHA domains characterized to date are highly selective for pThr-containing peptides. The pThr is the anchor residue for FHA-binding peptides[22], and dephosphorylation abrogates binding. The VHS domain differs from the FHA and the group IV WW domains in that the pSer enhances affinity but is not the central anchor for binding. The structures are consistent with this difference: in the WW and FHA domains, the phosphate makes extensive interactions with two or three of the nonbridging oxygens in a distinct pocket. In the GGA3 VHS–CI-MPR interaction, only one of the nonbridging phosphate oxygens is involved in direct interactions, and the site is exposed to the solvent. Thus, the GGA VHS domain belongs to a distinct class of binding modules that interact with phosphoserine-containing peptides preferentially but not exclusively.

Phosphoregulation of sorting signals

Taken together, our observations suggest that increased affinity resulting from phosphorylation underlies the requirement of Ser (-1) for efficient function of the CI-MPR in sorting lysosomal hydrolases[6]. We have yet to determine to what extent these findings apply to CD-MPR and other receptors recognized by the GGAs. A Ser residue within the acidic-cluster dileucine signal of the CD-MPR can also be phosphorylated *in vitro*[23] and *in vivo*[24]. This residue, however, is at position –4 relative to Asp 0 (Fig. 1*a*). Acidic-cluster dileucine signals from sortilin[9,17] and the low-density lipoprotein receptor-related protein 3 (LRP3)[9] also interact with the GGA VHS domains and contain Ser residues at positions –1 and –2, respectively, within putative CKII consensus sites (Fig. 1*a*). Examining whether phosphorylation of these Ser residues also modulates interactions with the GGA VHS domains will now be of interest.

The finding that phosphorylation regulates GGA-sorting receptor association adds to the class of phosphorylation events that regulate the interaction of sorting signals with their recognition molecules. CKII-mediated phosphorylation of an acidic cluster within the cytosolic tail of the endopeptidase furin allows binding to PACS-1, another adaptor protein that participates in retrieval of cycling proteins from endosomes to the TGN[25]. Similarly, phosphorylation of two Ser residues neighboring a dileucine-based signal from the T-cell co-receptor, CD4,

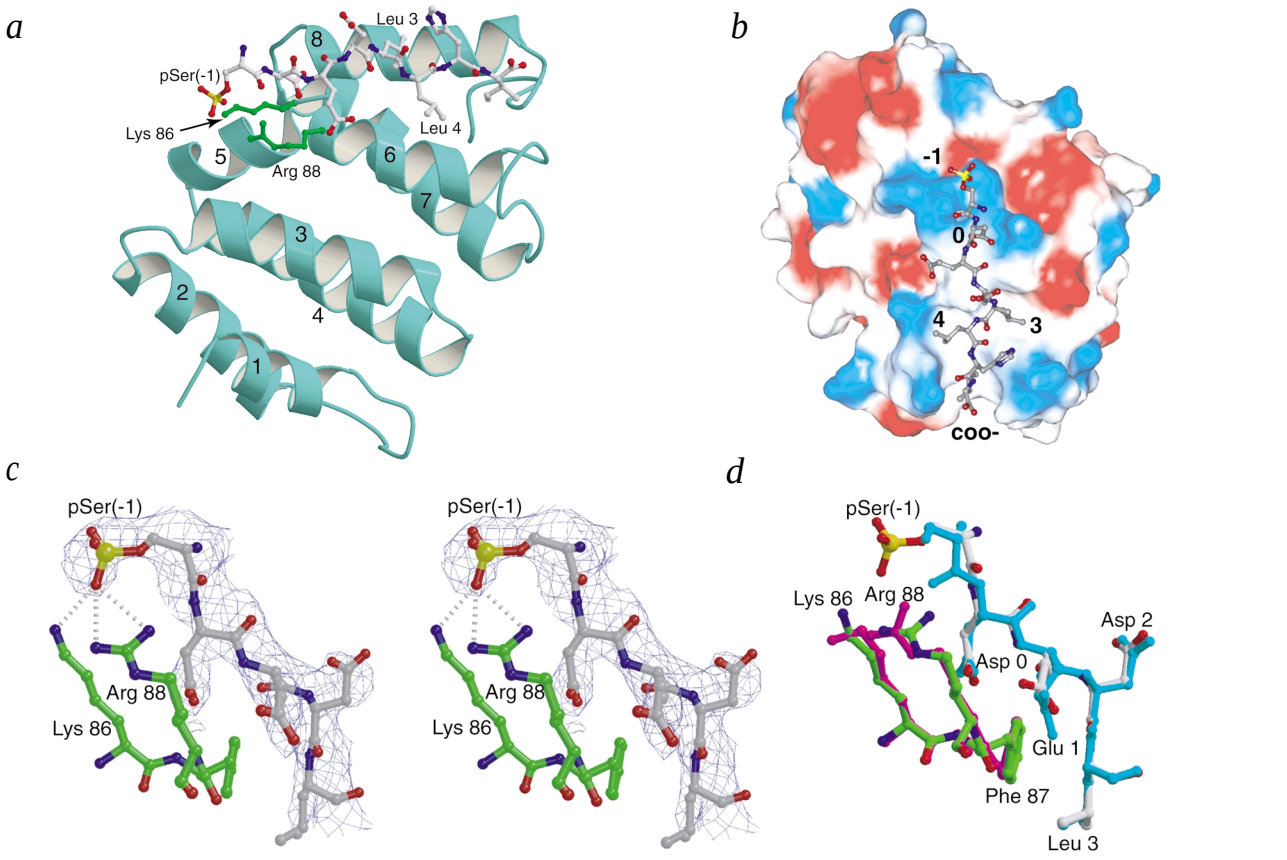

Fig. 4 Structure of the GGA3 VHS domain bound to phosphorylated CI-MPR peptide. ***a***, Overall architecture of the complex. The helices of the VHS domain are numbered. The peptide (CPK bonds) is bound between helices 6 and 8 of the VHS domain. The phosphoserine (pSer (-1)) and the two critical Leu residues (Leu 3 and Leu 4) of the peptide and the VHS residues that interact with the phosphoserine (Lys 86 and Arg 88) are labeled. ***b***, Surface electrostatics of the VHS domain with the bound CI-MPR phosphopeptide. The key pSer (-1), Asp 0, Leu 3 and Leu 4 residues and the C-terminus of the phosphopeptide are labeled. Saturated red and blue areas are at –10kT and +10kT, respectively. ***c***, Stereo view of the phosphoserine-binding site. The phosphopeptide residues have gray carbon bonds, and residues from the VHS domain are colored green The electron density for the phosphopeptide residues is shown as a SIGMAA-weighted $2mF_o - dF_c$ omit map (phosphopeptide omitted, map contoured at 0.9 σ). Interactions between the side chains of Lys 86 and Arg 88 and the phosphoserine are shown as dashed lines. ***d***, Superimposition of the first five residues of the CI-MPR peptide and residues 86–88 of the VHS domain in the phosphopeptide complex and the native peptide complex. The phosphopeptide and VHS domain residues from the phosphopeptide complex structure are colored as in (*c*). In the unphosphorylated peptide complex, the peptide and the VHS domain residues are colored magenta and cyan, respectively.

enhances interactions with the AP-1 and AP-2 clathrin adaptors[26]. The structural bases for these effects, however, remain to be explained. A different effect of signal phosphorylation has been described for tyrosine-based sorting signals conforming to the YXXΦ motif (Φ is a bulky hydrophobic amino acid residue). The T-cell co-receptor CTLA-4, for example, has an YXXΦ signal that interacts with the μ2 subunit of the AP-2 clathrin adaptor and mediates internalization of the unoccupied receptor[27]. Engagement by ligand triggers phosphorylation of the critical Tyr residue, but this precludes interaction with μ2 (ref. 27), presumably due to electrostatic repulsion by Asp 176 of μ2 (ref. 28). Thus, our findings provide the first structural insight into how phosphorylation of a sorting signal can positively regulate interactions with its cognate recognition protein.

Methods

Two-hybrid assays and metabolic labeling. Yeast cells were co-transformed with pGBT9(TRP) (Clontech) encoding GAL4bd fused to mutants of the last 113 amino acids of the CI-MPR cytosolic tail and the pGAD424(LEU2) vector encoding GAL4ad fused to different GGA VHS constructs. Co-transformed cells were cultured on plates lacking leucine and tryptophan, with or without histidine. Mutagenesis was performed using the QuikChange™ kit (Stratagene). For metabolic labeling, yeast cells were co-transformed with pGBKT7(TRP) encoding GAL4bd fused to an HA-tag and the CI-MPR tail, and pGAD424(LEU) encoding the GGA3 VHS domain. After overnight culture in medium lacking leucine, tryptophan and phosphate, cells (9×10^6 per sample) were labeled with 50 μCi ml^{-1} [^{32}P]orthophosphate for 3 h. Cells were lysed with glass beads and extracted with 50 mM Tris-HCl buffer, pH 7.5, containing 1% (w/v) SDS, 1 mM EDTA, 6 M urea and 10 mM each of vanadate, β-glycerophosphate and pyrophosphate.

Binding assays. For pull-down assays, GST fusion proteins (10 μg) were incubated with 0.24 units of CKII (Sigma) for 45 min at 37 °C in 40 mM HEPES buffer, pH 7.5, containing 1 mM ATP, 130 mM KCl, 10 mM $MgCl_2$ and 5 mM dithiothreitol (DTT). This was followed by incubation for 3 h at 4 °C with His_6–GGA3-VHS and glutathione–Sepharose 4B (50 μl) in PBS supplemented with 0.05% (v/v) Triton X-100. The beads were washed three times with PBS. Samples were analyzed by SDS-PAGE, followed by immunoblotting with antibody to the His_6-tag (Amersham-Pharmacia). For isothermal titration calorimetry, VHS domains were dialyzed into 100 mM NaCl, 50 mM phosphate buffer, pH 7.5, and 1 mM DTT and concentrated to 50 μM. The phosphorylated and unphosphorylated peptides were dissolved in the same buffer to 1 mM. Titration calorimetry measurements were performed using a MicroCal MCS-ITC instrument at 30 °C. Peptides were injected into 1.4 ml of GGA-VHS domains in 21

Table 1 Crystallographic data collection and refinement

Resolution range (Å)	50–2.3
R_{sym}[1–3]	0.062 (0.356)
Completeness[2,3]	96.1 (91.5)
R_{cryst}[2,4] (2.44–2.30 Å bin)	21.1 (26.4)
R_{free}[2,5] (2.44–2.30 Å bin)	25.5 (32.2)
Average B-factor (Å^2)	49.8
B-factor (Å^2) from Wilson plot	31.5
R.m.s. deviation	
Bond lengths (Å)	0.006
Bond angles (°)	1.3
Estimated coordinate error (Å)[6]	0.30
Number of atoms	
Total	5,277
Water	300
Residues in most favored region (%)	93.5
Ramachandran violations	0

[1]$R_{sym} = \Sigma_h\Sigma_i|I_i(h) - \langle I(h)\rangle| / \Sigma_h\Sigma_i I_i(h)$.
[2]Data in parentheses are for highest resolution shell.
[3]For all data (2.38–2.30 Å bin).
[4]R-factor $= \Sigma(|F_o| - k|F_c|) / \Sigma|F_o|$.
[5]R_{free} is the R-value calculated for a test set of reflections, comprising a randomly selected 10% of the data, not used during refinement.
[6]Determined using SIGMAA method.

aliquots of 10 μl each. Data obtained from peptide injections into 1.4 ml buffer blanks were subtracted from the corresponding experimental data before analysis using Origin 2.9 (MicroCal).

Crystallization and structure determination. The GGA3 VHS domain was expressed as a His_6-tagged fusion protein in *Escherichia coli* strain BL21(DE3) (Novagen) and purified by nickel affinity chromatography as described[15]. The purified domain contains the N-terminal residues Gly-Ala-Met-Gly-Gly-Ser, followed by human GGA3 residues 1–166. The protein was concentrated and dialyzed into crystallization buffer (50 mM NaCl, 20 mM Tris-HCl, pH 8.0, and 10 mM DTT). The phosphopeptide FHDDpSDEDLLHI was synthesized (New England Peptide) and added to the concentrated GGA3 VHS domain. The VHS/phosphopeptide mixture was diluted with crystallization buffer to final concentrations of 0.6 mM/1.5 mM, respectively. The VHS–phosphopeptide complex crystallized by vapor diffusion in 2 μl hanging drops over 0.5 ml reservoirs containing 100 mM 3-cyclohexylamino-1-propanesulfonic acid (CAPS), pH 10.2–11.0, 200 mM Li_2SO_4 and 1.4–1.7 M NaH_2PO_4/K_2HPO_4. A range of pH values and phosphate concentrations was always screened. Crystals grew over 3–7 d at 20 °C, up to $0.3 \times 0.3 \times 0.5$ mm in size. Crystals were cryoprotected by serial transfer into mother liquor supplemented with 5, 10, 15 and 20% (v/v) glycerol for 15–20 s per transfer. X-ray diffraction data were collected on crystals frozen directly in the cryostream. Data were collected using Cu Ka radiation from a Rigaku RU-200 rotating anode generator and a Rigaku RAXIS-IV detector with Osmic mirrors. Data were indexed and reduced as for the unphosphorylated complexes[15]. The crystals belonged to space group $C222_1$, with dimensions a = 124.54, b = 129.70, c = 108.58 Å and $\alpha = \beta = \gamma = 90°$. The coordinates of the GGA3-VHS domains from the structure of the GGA3-VHS–CD-MPR peptide complex (PDB entry 1JUQ), which has the same space group and similar unit cell dimensions, were used as an initial model for refinement against the collected data. Refinement was carried out in CNS[29] as for the unphosphorylated complexes[15]. Data collection and refinement statistics are shown in Table 1.

Coordinates. The coordinates have been deposited in the Protein Data Bank (accession code 1LF8).

Acknowledgments
We thank X. Zhu and E. Jones for expert technical assistance, and C. Arighi and M. Boehm for critical review of the manuscript.

Competing interests statement
The authors declare that they have no competing financial interests.

Correspondence should be addressed to J.H.H *email: jh8e@nih.gov* or J.S.B. *email: juan@helix.nih.gov*

Received 12 March, 2002; accepted 1 May, 2002.

1. Kornfeld, S. & Mellman, I. *Annu. Rev. Cell Biol.* **5**, 483–525 (1989).
2. Johnson, K.F. & Kornfeld, S. *J. Cell Biol.* **119**, 249–257 (1992).
3. Johnson, K.F. & Kornfeld, S. *J. Biol. Chem.* **267**, 17110–17115 (1992).
4. Chen, H.J., Remmler, J., Delaney, J.C., Messner, D.J. & Lobel, P. *J. Biol. Chem.* **268**, 22338–22346 (1993).
5. Mauxion, F., Le Borgne, R., Munier-Lehmann, H. & Hoflack, B. *J. Biol. Chem.* **271**, 2171–2178 (1996).
6. Chen, H.J., Yuan, J. & Lobel, P. *J. Biol Chem.* **272**, 7003–7012 (1997).
7. Puertollano, R., Aguilar, R.C., Gorshkova, I., Crouch, R.J. & Bonifacino, J.S. *Science* **292**, 1712–1716. (2001).
8. Zhu, Y., Doray, B., Poussu, A., Lehto, V.P. & Kornfeld, S. *Science* **292**, 1716–1718. (2001).
9. Takatsu, H., Katoh, Y., Shiba, Y. & Nakayama, K. *J. Biol. Chem.* **276**, 28541–28545 (2001).
10. Puertollano, R., Randazzo, P., Hartnell, L.M., Presley, J. & Bonifacino, J.S. *Cell* **105**, 93–102 (2001).
11. Pinna, L.A. *Biochim. Biophys. Acta* **1054**, 267–284 (1990).
12. Rosorius, O. *et al. Biochem. J.* **292**, 833–838 (1993).
13. Meresse, S., Ludwig, T., Frank, R. & Hoflack, B. *J. Biol. Chem.* **265**, 18833–18842 (1990).
14. Meresse, S. & Hoflack, B. *J. Cell Biol.* **120**, 67–75 (1993).
15. Misra, S., Puertollano, R., Kato, Y., Bonifacino, J.S. & Hurley, J.H. *Nature* **415**, 933–937 (2002).
16. Shiba, T. *et al. Nature* **415**, 937–941 (2002).
17. Nielsen, M.S. *et al. EMBO J.* **20**, 2180–2190 (2001).
18. Glover, C.V. III *Prog. Nucleic Acid. Res. Mol. Biol.* **59**, 95–133 (1998).
19. Yaffe, M.B. & Elia, A.E. *Curr. Opin. Cell Biol.* **13**, 131–138 (2001).
20. Fu, H., Subramanian, R.R. & Masters, S.C. *Annu. Rev. Pharmacol. Toxicol.* **40**, 617–647 (2000).
21. Verdecia, M.A., Bowman, M.E., Lu, K.P., Hunter, T. & Noel, J.P. *Nature Struct. Biol.* **7**, 639–643 (2000).
22. Durocher, D. *et al. Mol. Cell* **6**, 1169–1182 (2000).
23. Korner, C. *et al. J. Biol. Chem.* **269**, 16529–16532 (1994).
24. Hemer, F., Korner, C. & Braulke, T. *J. Biol. Chem.* **268**, 17108–17113 (1993).
25. Wan, L. *et al. Cell* **94**, 205–216 (1998).
26. Pitcher, C., Höning, S., Fingerhut, A., Bowers, K. & Marsh, M. *Mol. Biol. Cell* **10**, 677–691 (1999).
27. Shiratori, T. *et al. Immunity* **6**, 583–589 (1997).
28. Owen, D.J. & Evans, P.R. *Science* **282**, 1327–1332 (1998).
29. Brünger, A.T. *et al. Acta Crystallogr. D* **54**, 905–921 (1998).